GEOMETRY OF AXISYMMETRIC 3D ORIGAMI CONSISTING OF TRIANGLE FACETS

Yan ZHAO, Yoshihiro KANAMORI, and Jun MITANI
University of Tsukuba, Japan

ABSTRACT: Origami, the art of folding a piece of paper into a three-dimensional (3D) form, has received much attention in geometry, mathematics, and engineering. In recent years, several approaches for designing 3D origami have been proposed, and many creative origami pieces have been generated. In this paper, we propose a novel 3D origami design method for a new category of 3D origami that is constructed with triangle facets with axisymmetric structure. Our method interactively designs a rotationally-symmetric crease pattern and then analytically calculates the 3D origami model with real-time human interaction. The proposed method enables us to change one parameter to deform the 3D origami model while preserving the axisymmetric structure. By changing another parameter, our method leads to a way of folding a 3D origami model called "arc-direction flat-folding". By using our prototype system, we interactively explore various origami designs before actually making them. Several 3D origami pieces and folding sequences are presented to demonstrate the validity.

Keywords: Computational Origami, Axisymmetric, Deployable Structure, Flat-foldable.

1. INTRODUCTION

Origami, the art of folding a piece of paper into a three-dimensional (3D) form, has received much attention in geometry, mathematics, and engineering. In recent years, several approaches for designing 3D origami have been proposed, and many creative origami pieces have been generated.

In this paper, we propose a novel 3D origami design method for a new category of 3D origami that is constructed with triangle facets with axisymmetric structure. Our method interactively designs a rotationally-symmetric crease pattern (i.e., a set of creases on a surface that defines the structure of an origami piece) and then analytically calculates the 3D origami model with real-time human interaction.

Specifically, we first design the right part of the $1/N$ part ($N = 8$ for this example) of the whole crease pattern (Figure 1 (a)), where N indicates the order of rotational symmetry ($N > 2$) and the angle θ is determined by N, i.e., $\theta = 180^\circ/N$.

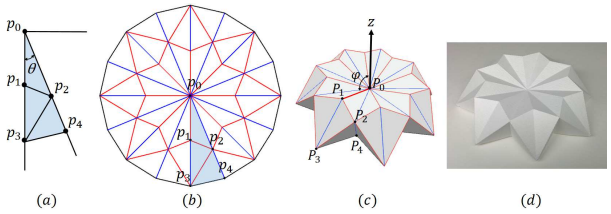

Figure 1: Overview of our method.

After the $1/N$ part has been specified, we generate the rotationally-symmetric crease pattern (Figure 1 (b)) by repeating such part $N-1$ times around the origin. Then, we use the crease pattern together with a user-specified value φ, which is the angle between line P_0P_1 and the z axis, to calculate a 3D origami model (Figure 1 (c)). Finally, based on the generated 3D model, we determine the mountain and valley assignments on the crease pattern, which are used to fold an origami piece (Figure 1 (d)).

We analyze the effects of variations by changing two parameters. By changing the angle φ and keeping the crease pattern fixed, we can deform

the 3D origami model while preserving developability and the axisymmetric structure. This enables us to figure out a folding motion from the fold-state to the flat-state of such a 3D origami model. By changing another parameter, our method leads to a way of folding a 3D origami model called "arc-direction flat-folding" based on the flat-foldability of each interior point verified by Kawasaki's theorem [4] and Maekawa's theorem [3] (Section 5.2). By using our prototype system, we interactively explore various origami designs before actually making them. Several 3D origami pieces and folding sequences are presented.

2. RELATED WORK

In recent years, origami has advanced significantly both in quantity and complexity based on the development of mathematical theories and more powerful computational resources [2, 13].

TreeMaker is software used to design flat-foldable origami [5]. This software generates the crease pattern from a graph tree that represents the base structure of the object by using the circle/river packing technique. *Tess* is a computer program that can make crease patterns for origami tessellations that involve twist folds in a repeating pattern [1]. These approaches focus on flat-foldable origami, but we are aiming at making 3D origami with a set of triangle facets.

The *Origamizer* algorithm, created by Tachi [12], is a very generalized approach that can generate a crease pattern for an arbitrary 3D triangle mesh model with topological disc condition. The basic idea is to place clearances between each polygon of the unfolded pattern and construct flaps from them inside the target shape; he called this "tucking". This method generates a crease pattern where the "tucks" are placed in the empty spaces so that the target 3D shape can be made from a single sheet of paper without requiring any cutting [10]. *Origamizer* can handle 3D rotational shapes; the appearance of the folded origami piece is equivalent to the target shape, but the generated pattern might be overly complicated for a simple model.

Mitani proposed a method for designing 3D origami based on rotational sweep [6] that generates a simpler crease pattern. Another of his methods [7] can generate 3D shapes that have 3D tucks with a triangular cross section. Although the outer flags might be considered obtrusive, his methods succeed in generating 3D curved origami from simple crease patterns. His method [8], which combines the advantages of the rotational sweep and mirror reflection approaches, has been used to build geometrically attractive origami pieces. Even though these methods can handle the axisymmetric structure of origami, it is difficult for them to handle the axisymmetric 3D origami consisting of triangle facets (Figures 1 and 12).

The interactive system is a creative and explorative tool for designers in computer-aided design (CAD) modeling and in 3D origami design. Tachi [11] proposed a design system where the user can intuitively vary a Miura-ori pattern in 3D while preserving the developability and other optional conditions inherent in the origami pattern. Another interactive system proposed by Mitani and Igarashi [9] allows the user to design 3D curved origami surfaces by using mirror operation with selecting and moving a vertex on the 3D origami while maintaining the developability of the resulting shape. In our work, the system implementing our method interactively designs a rotationally-symmetric crease pattern and then analytically calculates the 3D origami model with real-time human interaction.

3. DESIGNING CREASE PATTERN

In this section, we describe a rotationally-symmetric crease pattern consisting of triangle facets. The determination of mountain and valley assignments on a crease pattern based on the generated 3D origami model is described in Section 4.2.

Figure 2(a) shows a $1/N$ part of the crease pattern, and Figure 2(b) shows the shape in 3D space. The symbols in Figure 2 are as follows:

- Planes Π_1 and Π_2 are vertical planes whose intersecting lines cross the horizontal plane (i.e., the $x-y$ plane) are lines l_1 and l_2, respectively.
- P_0 is located at the origin in 3D space and expressed as p_0, indicating the intersection point of lines l_1 and l_2 on the horizontal plane.
- θ is the angle between lines l_1 and l_2, which equals $180^\circ/N$, and expressed as Θ in 3D space, indicating the angle between planes Π_1 and Π_2.
- P_1 and P_3 (with odd indices) lie on the plane Π_1 and represent p_1 and p_3 along line l_1 in the crease pattern, respectively.
- P_2 and P_4 (with even indices) lie on the plane Π_2 and represent p_2 and p_4 along line l_2 in the crease pattern, respectively.
- $P_2^{'}$ and $P_4^{'}$ (denoted as $p_2^{'}$ and $p_4^{'}$ in the crease pattern) are the symmetric points of P_2 and P_4 with respect to plane Π_1, respectively.

The rotationally-symmetric crease pattern can be interactively designed. Specifically, as shown in Figure 2 (a), the θ in the crease pattern can be changed by $N(N>2)$. $p_i(i>0)$ can be added or deleted along lines l_1 and l_2. Furthermore, $p_i(i>0)$ can be moved along lines l_1 or l_2. After the right part is specified, the symmetric points with respect to line l_1 are calculated. Finally, as shown in Figure 2 (c), the whole crease pattern is generated by repeating the $1/N$ part around the origin $N-1$ times by 2θ. The mountain and valley assignments are not determined until the 3D model is generated (Section 4.2).

4. CALCULATION OF EACH 3D POINT

In this section, we describe a method to calculate each point on the 3D origami model based on the crease pattern (using the example shown in Figure 1). P_0 is located at the origin in 3D space. Each 3D $P_i(i>0)$ is calculated sequentially in the order of its index. In Section 4.1, we describe the calculation of P_1 separately because a user-specified angle φ is needed. In Section 4.2, the calculation of $P_i(i>1)$ is described. In Section 4.3, a special case during calculation is given.

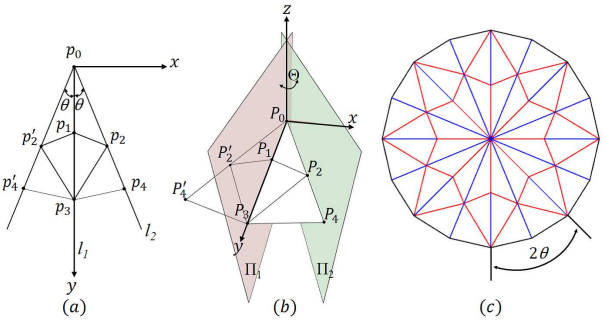

Figure 2: Designing rotationally-symmetric crease pattern consisting of triangle facets.

4.1 Calculation of P_1

To calculate the 3D coordinates of P_1, the following constraints should be satisfied:

1. The distance between P_1 and P_0 should be the same as the length of edge p_1p_0 in the crease pattern.
2. P_1 should lie on the plane Π_1.
3. Angle φ ($0^\circ \le \varphi \le 180^\circ$) between line P_0P_1 and the z axis should be the same as the user-specified value.

Figure 3 shows the process for calculating P_1. Firstly, considering constraint 1), the possible solutions for P_1 in 3D space lie on the red sphere (Figure 3 (a)) whose center is P_0 and radius equals the length of edge p_1p_0, which is measured from the crease pattern (Figure 1 (a)). Secondly, considering constraint 2), the possible solutions are shown as a red solution circle (Figure 3 (b) and (c)), which is the intersection between the red sphere and plane Π_1. Finally, by specifying the angle φ between line P_1P_0 and the z axis, the 3D coordinates of P_1 is determined. Figure 3 (b) and Figure 3 (c) show the solution of P_1 with $\varphi = 66^\circ$ and $\varphi = 140^\circ$, respectively. The angle φ is set to

66° and fixed throughout the subsequent calculation of the remaining 3D points.

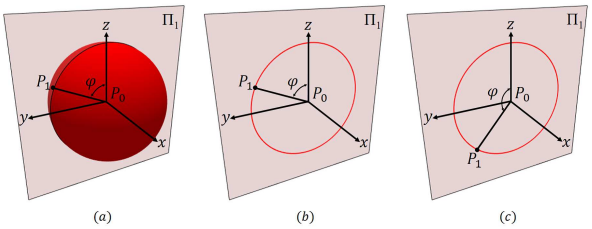

Figure 3: Calculation of P_1.

4.2 Calculation of $P_i (i > 1)$

In the sequential calculation of P_i, the 3D coordinates of P_{i-1} and P_{i-2} are required. For calculating $P_i (i > 1)$, the following three constraints should be satisfied:

1. The distance between P_i and P_{i-1} should be the same as the length of edge $p_i p_{i-1}$ in the crease pattern.

2. The distance between P_i and P_{i-2} should be the same as the length of edge $p_i p_{i-2}$ in the crease pattern.

3. P_i should lie on the plane Π_1 (for odd index) or Π_2 (for even index).

For generating $P_i (i = 2)$ (Figure 4), the 3D coordinates of P_1 and P_0 are required. In Figure 4 (a) and (b), we first consider constraint 1) between P_i and P_{i-1} (i.e., P_2 and P_1 in this example). The possible solutions for P_2 in 3D space lie on a sphere, called a solution sphere, whose center is P_1 and radius equals the length of edge $p_2 p_1$. Then, by considering constraint 3), the solution circle shown in red is obtained from the previous solution sphere intersected by plane Π_2. Next, by considering constraint 2) between P_i and P_{i-2} (i.e., P_2 and P_0) and constraint 3), we obtain the solution circle shown in green on plane Π_2 whose center is P_0 and radius equals the length of edge $p_2 p_0$. Finally, the two intersection points between the two solution circles (the red one and the green one) that satisfy all the constraints at

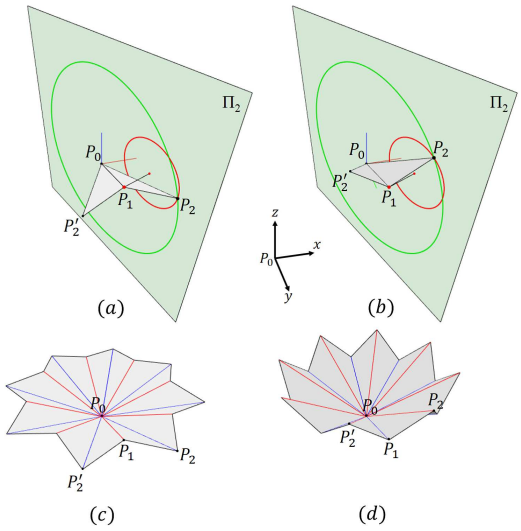

Figure 4: Calculation of $P_i (i = 2)$.

the same time are selected as two candidate solutions for $P_i (i = 2)$. For the solution of P_2(with even index), the symmetric point P_2' with respect to plane Π_1 is calculated.

After the $1/N$ part of the 3D origami model is specified, the whole 3D origami model is generated by repeating the part around the z axis $N-1$ times by 2Θ as shown in Figure 4 (c) and (d), respectively.

The calculation process of $P_i (i = 3)$, which lies on plane Π_1, is shown in Figure 5. By satisfying all the constraints, the two intersection points of the two solution circles on plane Π_1 are selected as candidate solutions for $P_i (i = 3)$ (Figure 5 (a) and (b)). For designing various shapes of 3D origami, either candidate can be selected as the solution of P_3 (Figure 5 (c) and (d)). However, one solution could flatten two connected facets (Figure 5 (d)); thus, the crease lines between such flattened facets are rendered in green.

We also show the calculation for $P_i (i = 4)$, which lies on plane Π_2, with the constraints from P_3 and P_2 (Figure 6). The shape (Figure 6(c)) is the 3D model introduced in Figure 1(c). We determine the mountain and valley assignments on a 3D model and then translate them to crease patterns (Figure 1 (b)).

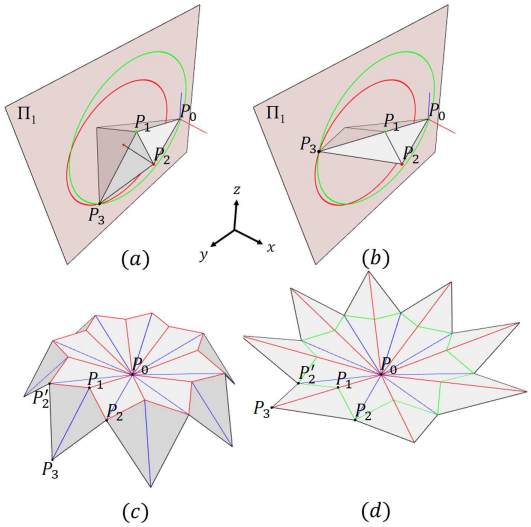

Figure 5: Calculation of $P_i(i = 3)$.

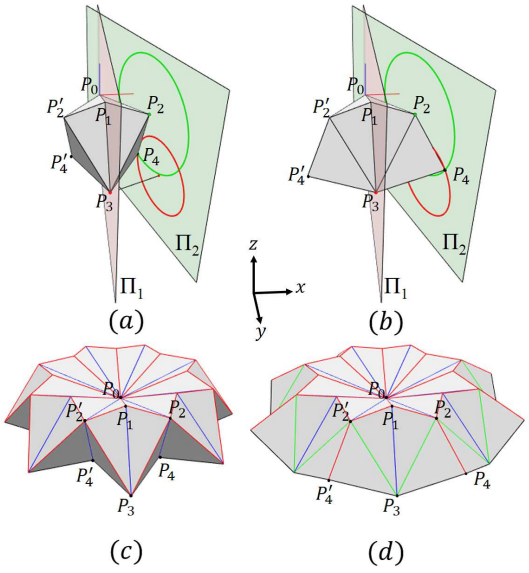

Figure 6: Calculation of $P_i(i = 4)$

4.3 Special Case in Calculation of $P_i(i > 1)$

The candidate solutions for each $P_i(i > 1)$ are two intersection points of the two solution circles as described in Section 4.2. A special case occurs when the two solution circles are identical. Then, the candidate solutions for $P_i(i > 1)$ are not just two points but all the points along the solution circle.

Figure 7 shows one example of the special case for calculating P_3, where $\varphi = 90°$ and line

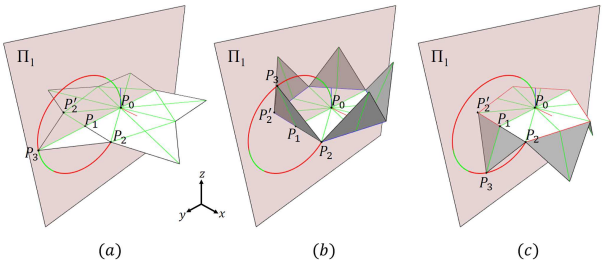

Figure 7: Special case in calculation.

P_2P_1 is vertical to plane Π_1. In such a case, the solution circle shown in red is constructed by points that satisfy constraints 1) and 3). The other solution circle shown in green is constructed by the points that satisfy constraint 2) and 3). Both circles share the same center P_1 and have the same radius, which is the length of edge p_3p_1. As a result, the candidate solutions for P_3 in this case are not just two points but all the points along the solution circle. In Figure 7, P_3 can be selected arbitrarily on the solution circle to design various 3D origami models.

5. EFFECTS ON GEOMETRY

In this section, we analyze the effects of variations by changing the parameters including angle φ (Section 5.1) and angle Θ (Section 5.2).

5.1 Changing angle φ

The 3D origami model is a developable surface that is isometric, which means that the distance between two points on the flat undeveloped plane will be equivalent to the distance between the two corresponding points on the developed surface. In this section, benefit the process of generating the 3D origami model that are

1. The change in angle φ only affects P_1 directly.

2. Each subsequent $P_i(i > 1)$ is to be recalculated sequentially, which means P_i is not recalculated until the previous P_{i-1} and P_{i-2} have been recalculated.

3. Each $P_i(i > 1)$ is recalculated based on P_{i-1}

and P_{i-2}, which have already been recalculated.

, we are able to change only angle φ, and the resulting surface remains developablility.

The user can explore various origami models by only changing angle φ. Figure 8 shows some possible shapes of origami model. We set φ to 66° (Figure 8 (b)) to obtain the shape we introduced in Section 1. Figure 8 (d) shows that the 3D origami model can be completely unfolded just the same as the 2D crease pattern. With angle φ set from 66° to 90°, we can figure out a folding motion that shows the change from the fold-state to the unfold-state of such a 3D origami model.

Although φ can theoretically be from 0° to 180°, penetration between triangle facets could happen at some values of φ (Figure 8 (a), (g), and (h)). We leave it up to the user in the designing process to avoid such illegal values of φ to generate real-world origami pieces.

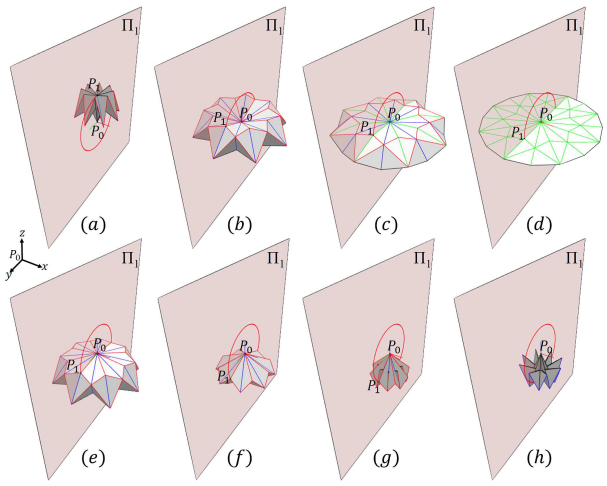

Figure 8: Various origami designs obtained by changing φ from 0° to 180°: (a) $\varphi = 0^\circ$, (b) $\varphi = 66^\circ$, (c) $\varphi = 83^\circ$, (d) $\varphi = 90^\circ$, (e) $\varphi = 97^\circ$, (f) $\varphi = 115^\circ$, (g) $\varphi = 135^\circ$, (h) $\varphi = 180^\circ$.

5.2 Changing angle Θ

Θ denotes the angle between planes Π_1 and Π_2 in 3D space, which equals $180^\circ/N$. After the $1/N$ part of the origami model is calculated, the whole origami model is generated by repeating the part around the z axis $N-1$ times by 2Θ.

In this section, we decrease Θ, expressed as Θ', from $180^\circ/N$ to 0°. By inserting an extra boundary line in the crease pattern, we keep the property of developablility of the 3D model during the decreasing of angle Θ'. Then, we verify the flat-foldability of each interior point on the crease pattern by Kawasaki's theorem and Maekawa's theorem, leading to a way of folding called "arc-direction flat-folding".

Specifically, first, we decrease Θ to Θ' and then use Θ' to generate the $1/N$ part of the origami model. Note that such a $1/N$ part still maintains a developable surface as each 3D edge is equivalent to the corresponding edge on the flat undeveloped plane (crease pattern).

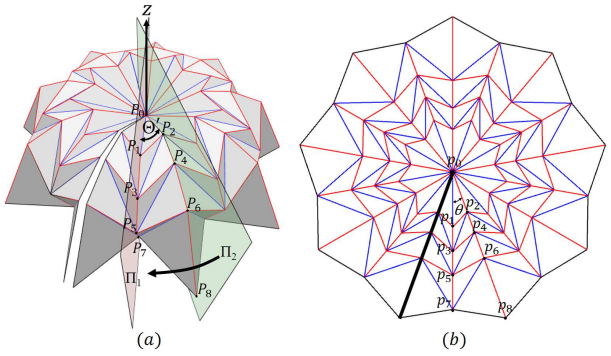

Figure 9: Maintain developable property of 3D model.

Then, we repeat the $1/N$ part around the z axis $N-1$ times by $2\Theta'$ to generate the whole origami model (Figure 9 (a)). Note that the last $1/N$ part is separated from the first $1/N$ part, which breaks the developable property of the 3D model. In this situation, we insert a boundary line in the crease pattern (Figure 9 (b)) to maintain the developable property of the whole 3D model.

The process of decreasing angle Θ' makes P_i (with even indices) on plane Π_2 together with the symmetric P_i' fall towards plane Π_1. For the whole 3D model, such a process compresses the 3D origami model towards plane Π_1.

Here, we check the flat-foldability of the 3D

origami model by verifying the flat-foldability of each interior point using Kawasaki's theorem and Maekawa's theorem. Kawasaki's theorem gives a criterion for an origami construction to be flat, which states that a given crease pattern can be folded to a flat origami iff all the sequences of angles $\alpha_1, \alpha_2, \cdots, \alpha_{2n}$ surrounding each interior vertex fulfill the following condition: $\alpha_1 + \alpha_3 + \cdots + \alpha_{2n-1} = \alpha_2 + \alpha_4 + \cdots + \alpha_{2n} = 180^\circ$. Maekawa's theorem is another criterion, which states that the numbers of mountains and valleys always differ by 2. Kawasaki's theorem and Maekawa's theorem are two local flat-foldable conditions.

We show one middle state of the 3D model for decreasing Θ' in the left of Figure 10. Note that the 3D origami model preserves the developability with respect to the updated crease pattern (Figure 9 (b)); thus, the surrounding crease of each interior point is fixed during the decreasing of Θ' to 0°.

Without loss of generality, we verify the flat-foldability of the interior points by showing the details of the crease pattern around P_1 and P_4, which lie on the planes Π_1 and Π_2, respectively. Angle $\alpha_{i,k}$ denotes the $k-$th incident sector angle of p_i as shown on the right of Figure 10. Here, we do not consider p_0 since the added boundary line makes p_0 a boundary point (Figure 9 (b)). Specifically, for P_1, since $\alpha_{1,1} = \alpha_{1,2}$ and $\alpha_{1,3} = \alpha_{1,4}$ and thus $\alpha_{1,1} + \alpha_{1,3} = \alpha_{1,2} + \alpha_{1,4} = 180^\circ$, which satisfies Kawasaki's theorem. Also, since the number of mountain lines (3) minus the number of valley lines (1) equals 2, Maekawa's theorem is satisfied. Similarly, for P_4, since $\alpha_{4,1} = \alpha_{4,2}$, $\alpha_{4,3} = \alpha_{4,6}$ and $\alpha_{4,4} = \alpha_{4,5}$, and thus $\alpha_{4,1} + \alpha_{4,3} + \alpha_{4,5} = \alpha_{4,2} + \alpha_{4,4} + \alpha_{4,6} = 180^\circ$, which satisfies Kawasaki's theorem. Also, since the number of mountain lines (4) minus the number of valley lines (2) equals 2, Maekawa's theorem is satisfied.

If all interior points satisfy Kawasaki's theorem and Maekawa's theorem, we can decrease Θ' to 0° to fold the whole 3D model around the z axis (Figure 11), which is a way of folding called

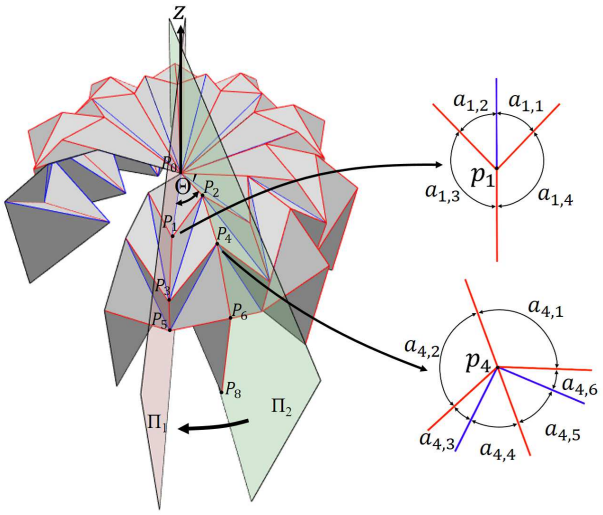

Figure 10: Check flat-foldability with Kawasaki' theorem and Maekawa's theorem.

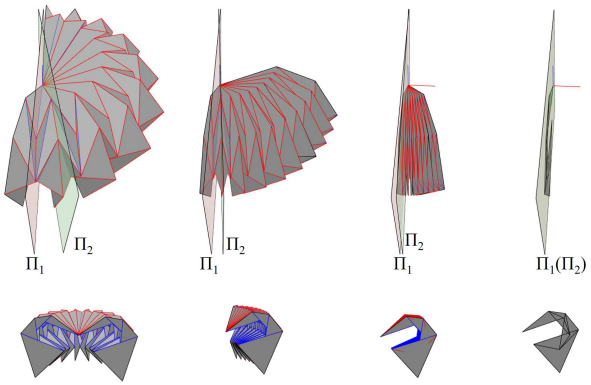

Figure 11: Arc-direction flat-folding sequence.

"arc-direction flat-folding".

6. RESULTS

We show several resulting origami pieces in Figure 12, where the first row is the crease pattern, the second row is the 3DCG model, and the third row is the photo of the origami piece.

Figure 12 (a), (b), and (c) show the 3D origami pieces constructed with triangle facets. By applying the special case, we design origami pieces that have both a flat center area and triangle facets, as shown in Figure 13. In Figure 14, we show the folding motion of the origami models from the fold-state to the flat-state (Figure 12 (a), (b), and (c)) by changing parameter φ.

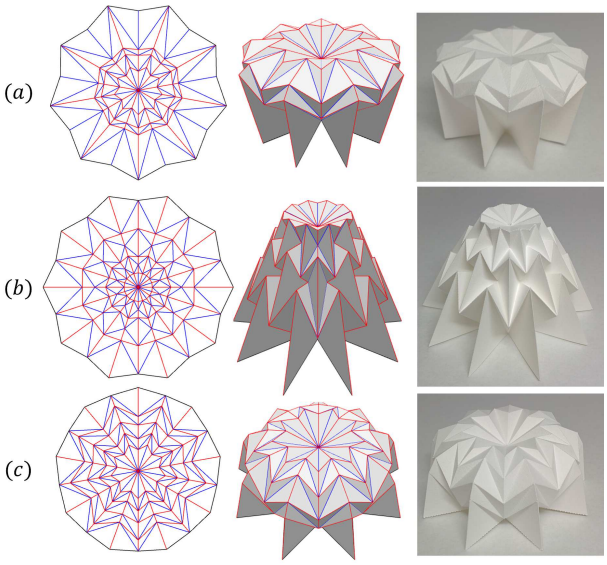

Figure 12: Resulting origami pieces with triangle facets.

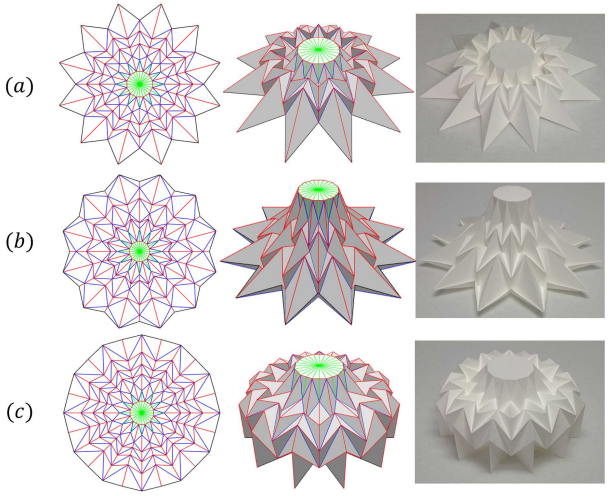

Figure 13: Resulting origami pieces with flat center area and triangle facets.

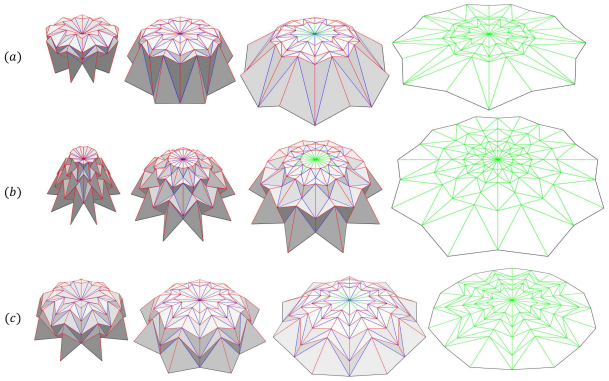

Figure 14: Flat-folding motions.

Figure 15 shows the "arc-direction flat-folding" of the origami model shown in Figure 12 (b) and (c). The photo of the real origami pieces and the folded shapes are shown in Figure 16.

7. CONCLUSION

We have described a design method for a new category of 3D origami constructed with triangle facets with axisymmetric structure. We focused on the property of axisymmetric structure to introduce a rotationally-symmetric crease pattern and then described the details of the calculation of each point on a 3D origami model. For the calculation of $P_i(i > 1)$, the two intersection points of the solution circles were selected as solution candidates for $P_i(i > 1)$. Each of them was used to create different 3D models. During the calculation, we found a special case where the two solution circles are identical; thus, the candidate solutions are not two points but all the points on the solution circle. We have applied the special case in designing origami pieces with a flat center.

We analyzed the effects of variations by changing two parameters: angle φ and Θ. First, we changed φ, which is the angle between the edge P_0P_1 and the z axis. The benefit of the process of generating the 3D origami model is, for each updated φ, the updated model remains developability. This enables us to explore various origami designs and figure out a folding motion from the fold-state to the flat-state of such a 3D origami model.

Next, we introduced a way of folding called "arc-direction flat-folding" by changing the value of Θ, which is the angle between planes Π_2 and Π_1, from $180^\circ/N$ to 0°. To keep consistency between the crease pattern and the 3D model during the process of decreasing Θ, we inserted a boundary line in the crease pattern. Then, we checked the flat-foldability of the 3D origami model by

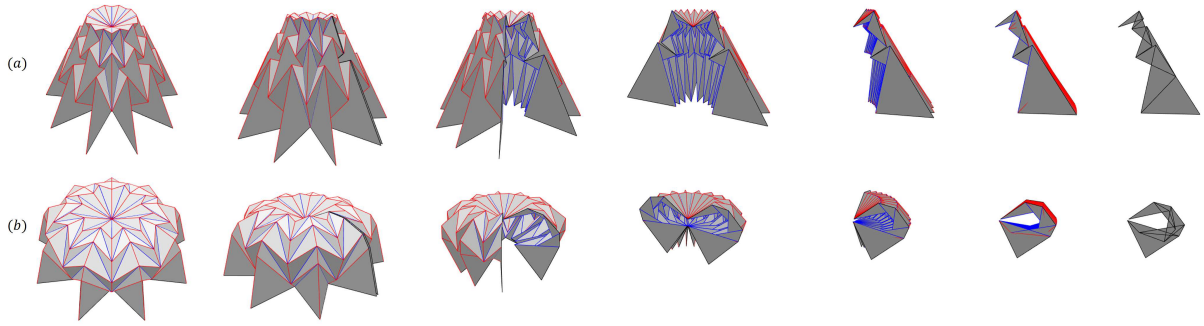

Figure 15: Arc-direction flat-folding sequences.

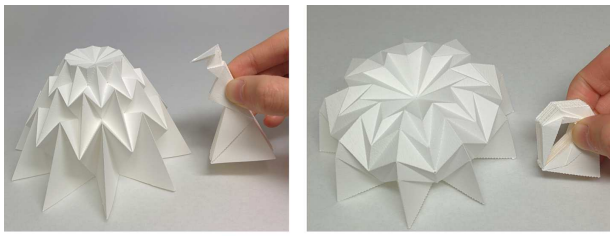

Figure 16: Arc-direction flat-folding of real origami pieces.

verifying the flat-foldability of each interior point using Kawasaki's theorem and Maekawa's theorem. We showed the "arc-direction flat-folding" sequences and practiced such folding in real origami pieces.

One future work is to use tuck folding technology to design axisymmetric 3D origami consisting of triangle facets.

REFERENCES

[1] A. Bateman. Paper mosaic origami tessellations. `http://www.papermosaics.co.uk/software.html`.

[2] E. D. Demaine and J. ORourke. *Geometric folding algorithms*. Cambridge university press Cambridge, 2007.

[3] K. Kasahara and J. Maekawa. Viva! origami, 1983.

[4] T. Kawasaki. On the relation between mountain-creases and valley-creases of a flat origami. In *Proceedings of the 1st International Meeting of Origami Science and Technology*, pages 229–237. 1989.

[5] R. J. Lang. Treemaker. *Robert J. lang Origami*, 2006. `http://www.langorigami.com/article/treemaker/`.

[6] J. Mitani. A design method for 3D origami based on rotational sweep. *Computer-Aided Design and Applications*, 6(1): 69–79, 2009.

[7] J. Mitani. A design method for axisymmetric curved origami with triangular prism protrusions. In *Origami 5: Fifth International Meeting of Origami Science, Mathematics, and Education*, page 437. CRC Press, 2011.

[8] J. Mitani. Column-shaped origami design based on mirror reflections. *Journal for Geometry and Graphics*, 16(2): 185–194, 2012.

[9] J. Mitani and T. Igarashi. Interactive design of planar curved folding by reflection. *Pacific Graphics (short paper)*, 2011.

[10] T. Tachi. 3D origami design based on tucking molecule. In *The Fourth International Conference on Origami in Science, Mathematics, and Education, R. Lang, ed., Pasadena*, pages 259–272. 2009.

[11] T. Tachi. Freeform variations of origami. *J. Geom. Graph*, 14(2): 203–215, 2010.

[12] T. Tachi. Origamizing polyhedral surfaces. *Visualization and Computer Graphics, IEEE Transactions on*, 16(2): 298–311, 2010.

[13] P. Wang-Iverson, R. J. Lang, and Y. Mark. *Origami 5: Fifth International Meeting of Origami Science, Mathematics, and Education*. CRC Press, 2011.

ABOUT AUTHORS

1. Yan Zhao, Ph.D. student at the Department of Computer Science, University of Tsukuba.

2. Yoshihiro Kanamori, Assistant Professor at the Department of Computer Science, University of Tsukuba.

3. Jun Mitani, Professor at the Department of Computer Science, University of Tsukuba.